Advanced Ceramics Progress: Vol. 10, No. 3, (Summer 2024) 15-22

Materials and Energy Research Center
MERC

Contents lists available at ACERP
Advanced Ceramics Progress
Journal Homepage: www.acerp.ir

Original Research Article

Optical Properties of Flexible Nanocomposites Synthesized as Powders via the Hydrothermal Method Under Ionizing Excitations

Danial Moradi [a], Mona Hosseini [a], Maryam Hajiebrahimi [b], Sanaz Alamdari [c]*, Omid Mirzaee [d]*

[a] *BSc Student, Faculty of Materials and Metallurgical Engineering, Semnan University, Semnan, Iran.*
[b] *Research Assistant, Faculty of Materials and Metallurgical Engineering, Semnan University, Semnan , Iran.*
[c] *Assistant Professor, Department of Nanotechnology, Faculty of New Sciences and Technologies, Semnan University, Semnan, Iran.*
[d] *Professor, Faculty of Materials & Metallurgical Engineering, Semnan University, Semnan, Iran.*

* Corresponding Author Email: s.alamdari@semnan.ac.ir (S. Alamdari), o_mirzaee@semnan.ac.ir (O. Mirzaee);
URL: https://www.acerp.ir/article_211267.html

A R T I C L E I N F O

Article History:
Received: 31 November 2024
Revised: 14 December 2024
Accepted: 22 December 2024

Keywords:
$CdWO_4$
Silver Dopant
Co-precipitation
Nanoparticles
Scintillation Properties

A B S T R A C T

In this study, cadmium tungstate ($CdWO_4$) and silver-doped cadmium tungstate ($CdWO_4$:Ag)/polyvinyl alcohol (PVA) nanocomposite films were successfully fabricated. The preparation of the nanocomposite films was accomplished through a straightforward hydrothermal procedure following an established protocol. XRD, EDX, and Fourier-transform infrared (FTIR) spectroscopy confirmed the successful synthesis of $CdWO_4$ and $CdWO_4$:Ag nanopowders. FESEM images revealed mean particle sizes of approximately 345 nm for $CdWO_4$ and 267 nm for $CdWO_4$:Ag nanopowders, respectively. The luminescence characteristics of the synthesized nanoparticles were evaluated under UV irradiation. The $CdWO_4$:Ag nanoparticles exhibited significantly higher luminescence intensity within the blue-green spectrum compared to the pure $CdWO_4$ sample. The radiative response of the samples was meticulously assessed using an (^{241}Am) alpha source, with the doped sample demonstrating a marked improvement in the count rate compared to the $CdWO_4$ composite. Furthermore, the $CdWO_4$:Ag composite exhibited acceptable counting efficiency, performing at levels comparable to more expensive alpha counters. These findings suggest that the $CdWO_4$:Ag/PVA nanocomposite holds significant potential as an effective scintillation material optimized for radiation detection applications.

https://doi.org/10.30501/acp.2024.486443.1166

1. INTRODUCTION

Nowadays, the demand for radiation detection technology in medical and industrial sectors is substantial. Thermoluminescent dosimeters (TLDs) and ionizing radiation detectors (scintillators) are critical and highly regarded analytical devices across various medical professions (Alamdari et al, 2022; Dehkordi.N et al, 2022). Traditional inorganic and organic scintillators face limitations due to high manufacturing costs and inadequate responsiveness to varying environmental conditions. For example, single crystals are frequently employed in the fabrication of highly efficient luminescent materials for optical technologies (Alamdari.S et al, 2020). Nevertheless, this method encounters inherent challenges, including the introduction of various defects during crystal growth and the potential for cracking after cooling to ambient temperature (Alamdari et al, 2022; Hosseinpour et al, 2023; Alamdari.S et al, 2021; Alamdari et al, 2020; Wang, X. et al, 2022). Consequently, it is imperative to develop

Please cite this article as: Moradi, D., Hosseini, M., Hajiebrahimi, M., Alamdari, S. & Mirzaee, O. (2024). Optical Properties of Flexible Nanocomposites Synthesized as Powders via the Hydrothermal Method Under Ionizing Excitations, *Advanced Ceramics Progress*, 10(3), 15-22. https://doi.org/10.30501/acp.2024.486443.1166

scintillator nanopowders that can be produced through cost-effective methods and adapted into various forms, such as flexible films within polymeric matrices (Alamdari.S et al, 2022). Currently, research on materials that integrate polymers with inorganic components to enhance luminescence and flexibility is gaining significant traction among scientists (Azadmehr et al, 2022; Hemmati et al, 2022; Alamdari et al, 2022). Over the past three decades, a diverse array of oxide-derived semiconductors exhibiting significantly enhanced luminescent characteristics has undergone extensive development, aiming to attain superior performance in various luminescent apparatuses (Alamdari.S et al, 2025; Alamdari.S et al, 2019). Oxide-derived semiconductor materials have garnered considerable attention owing to their extensive potential for commercial use in display technology, LEDs, and scintillation devices (Hosseinpour et al, 2022; Dehkordi.N et al, 2024). Tungstate compounds exemplify luminescent materials that are increasingly captivating interest within the industry, attributed to their numerous advantageous properties and excellent physical and chemical characteristics (Dehkordi et al, 2022; Ziluei et al, 2017). Among them, cadmium tungstate ($CdWO_4$, CWO) stands out as one of the most esteemed scintillation materials for a broad spectrum of technological applications. This acclaim is attributed to its exceptional stopping power, high efficacy, and impressive chemical resilience. It is a prominent n-type semiconducting material, characterized by a narrow band gap of 3.28 eV at room temperature. $CdWO_4$ is well-established to exhibit polymorphic forms: the monoclinic wolframite phase and the tetragonal scheelite structure, both of which are contingent upon specific preparation conditions. Owing to these properties, $CdWO_4$ is intrinsically interesting for quantum technologies (Dehkordi et al, 2022; Dehkordi et al, 2022; Sahani et al, 2019).

Incorporating diverse inorganic or organic components into oxide materials can effectively alter their optical characteristics (Alamdari.S et al, 2019). For example, photosensitivity may be significantly enhanced through Förster resonance energy transfer (FRET) mechanisms between the polymer matrix and nanostructured fillers within the pliable nanocomposite (Alamdari et al, 2022; Murphy et al, 1999; Hajiebrahimi et al, 2022). Doping and bandgap engineering are generally two key strategies for improving the quantum performance of semiconductor materials (Alamdari.S et al, 2021). The luminescence properties and optical characteristics of substances can be significantly enhanced through doping or by integrating dual oxide semiconductors (Madani.M et al, 2022). This innovative approach leads to the creation of novel nanocomposites endowed with appropriate energy band levels and unique properties (Alamdari et al, 2022; Dehkordi et al, 2022; Dehkordi et al, 2022). A recent study revealed that the readily fabricated $ZnO/CdWO_4$:Ce nanocomposite exhibited exceptional sensitivity when subjected to UV, proton, and alpha radiation exposure (Alamdari et al, 2022; Tafreshi et al, 2022.). In an alternative methodology, Ou et al. engineered a flexible radiation detector by incorporating $NaLuF_4$:Tb @$NaYF_4$ nanoparticles within a polydimethylsiloxane (PDMS) matrix (Banari et al, 2023). Hemmati et al. documented the development of a highly sensitive and adaptable ionizing radiation detector utilizing a composite $BaWO_4$-chitosan-based nanocomposite (Xu et al, 2020). Additionally, dopants or activators can introduce significant changes in the regular crystal lattice of semiconductors. The specific role of each dopant is pivotal to the efficiency of device performance (Dehkordi.N et al, 2022). Ag, as a promising dopant in $CdWO_4$, acts as a shallow-level donor surface, providing sufficient electrons to enhance optical properties. The desired optical characteristics can be readily achieved by adding Ag as a dopant (Alamdari et al, 2022; Alamdari et al, 2025).

In this study, $CdWO_4$ and $CdWO_4$:Ag nanoparticles were successfully fabricated using a simple chemical method and embedded in PVA thin films, which is significantly more straightforward than relying on crystal growth methods. The doped specimen exhibited unique sensitivity and optical characteristics in response to alpha irradiation at room temperature, indicating its potential as a viable candidate for photonic applications.

2. MATERIALS AND METHODS

2.1. REAGENTS

Sodium tungstate dihydrate ($Na_2WO_4 \cdot 2H_2O$) and cadmium acetate dihydrate ($Cd(CH_3COO)_2 \cdot 2H_2O$) powders, as two precursors of cadmium tungstate ($CdWO_4$), along with silver nitrate ($AgNO_3$), were sourced from Sigma-Aldrich and utilized immediately without any additional purification steps.

2.2. SYNTHESIS OF CWO NPs

The hydrothermal technique was employed to synthesize CWO:Ag nanoparticles. In this context, 5 grams of sodium tungstate dihydrate and 5 grams of cadmium acetate dihydrate and 2 cc TEA were individually dissolved in 50 mL of distilled water at ambient temperature using a magnetic stirrer for 30 minutes. The sodium tungstate dihydrate solution was then added to the cadmium acetate dihydrate solution. The mixture was continuously stirred for 1 hour, after which silver nitrate (2 at.%) was added to the suspension under constant stirring for 30 minutes. The resulting suspension was transferred to a Teflon-lined stainless steel autoclave and sealed. The autoclave was heated to 180°C and maintained at this temperature for 12 hours to allow the hydrothermal reaction to proceed. After cooling to room temperature naturally, the resulting cadmium tungstate solution was collected, washed, and then dried in an oven at 80°C for 24 hours. Finally, the nanopowders were calcined by heating the sample in a furnace at a specific temperature of 600°C for 3 hours. The synthesis process of the CWO:Ag nanopowders is illustrated in Figure 1.

2.3. CHARACTERIZATION

To ascertain the crystalline structure and phase composition of the material, X-ray diffraction (XRD) analysis was conducted using the Bruker D8-Advance system. The morphology and elemental composition of the materials were meticulously analyzed using field emission scanning electron microscopy (FESEM-TESCAN). Fourier-transform infrared (FTIR) spectroscopy, utilizing a PerkinElmer instrument, was employed to examine the functional groups and vibration modes present in the materials. To investigate the characteristic properties, UV-visible diffuse reflectance spectroscopy (Perkin-Elmer LS-5) was employed. To explore the radiation response of the samples, flexible $CdWO_4$ films were paired with a photomultiplier (Model FEU_31, Russia) using optical grease. Subsequently, the count rates were measured using collimated rays from a ^{241}Am alpha source, with an activity of 0.09 µCi.

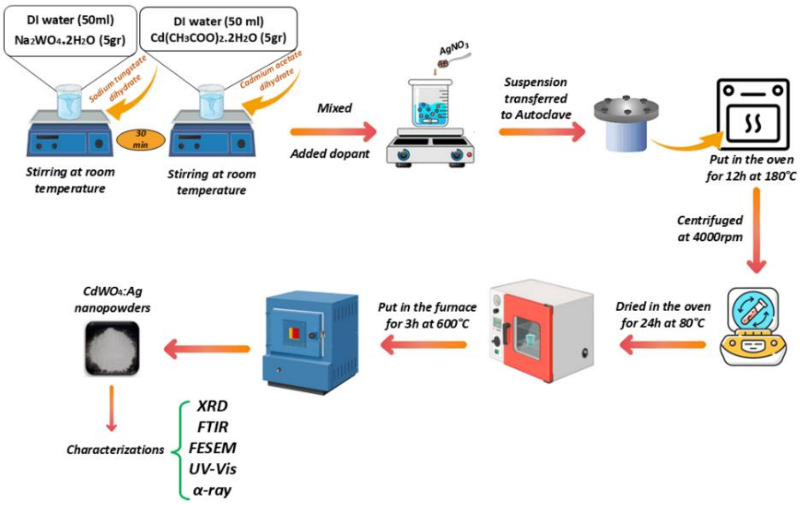

Figure 1. Brief schematic of the experimental works

3. RESULTS AND DISCUSSION

3.1. X-RAY DIFFRACTION (XRD)

The X-ray diffraction (XRD) profiles of both pure and silver-doped $CdWO_4$ are presented in Fig. 2(a). The XRD peaks of the $CdWO_4$ sample revealed primary peaks consistent with the standard data for the monoclinic structure of $CdWO_4$ (CWO) (JCPDS card no. 00-013-0514). No impurity phases were detected when silver ions (Ag^+) were incorporated into the $CdWO_4$ host lattice. The ionic radius of Ag^+ (r = 1.29 Å) closely aligns with that of cadmium ions (Cd^{2+}) (r = 1.09 Å) and is substantially larger than that of tungsten ions (W^{6+}) (r = 0.60 Å), suggesting a preferential substitution of Ag^+ ions at Cd^{2+} sites. As shown in Fig. 2(b), the highest intensity diffraction peaks of the (-111) and (111) lattice planes, present in both samples, fall within the angular range of 28° to 30°. The (-111) and (111) peaks in Ag^+-doped $CdWO_4$ exhibited a subtle shift towards a higher angular direction, attributable to the larger ionic radius of Ag^+ compared to Cd^{2+}. Additionally, the diffraction peak intensities in Ag-doped $CdWO_4$ were slightly increased compared to $CdWO_4$ (CWO). This enhancement is attributed to the effective substitution of Ag^+ ions for Cd^{2+} sites and the resulting high crystallinity (Alamdari et al, 2022; Hajiebrahimi et al, 2022). The crystallite sizes of $CdWO_4$ and Ag-doped $CdWO_4$ nanoparticles were determined using X-ray line broadening, applying Scherrer's formula as shown in equation (1):

$$D = \frac{K\lambda}{\beta cos\theta} \tag{1}$$

where D denotes the average crystalline size, k the shape factor (0.9), λ the wavelength of the incident X-ray beam, θ the Bragg's diffraction angle, and β the full width at half maximum intensity of the peak (Hosseinpour et al, 2023). The mean crystallite size (grain size) of the undoped and Ag-doped

$CdWO_4$ samples, calculated from the most intense peaks based on the Scherer formula, is summarized in Table 1. It shows the average particle size obtained from the Scherrer formula for CWO and Ag-doped CWO nanoparticles, which range from 30 to 40 nm.

Table 1. The average particle size of $CdWO_4$ and Ag-doped $CdWO_4$ nanopowders

Sample	Peak position (°)	FWHM	D (nm)
$CdWO_4$	23.3753	0.2558	40.86
	29.0767	0.1919	
	29.6518	0.1919	
$CdWO_4$: Ag	23.4553	0.2558	34.93
	29. 2343	0.1919	
	29.7679	0.1919	

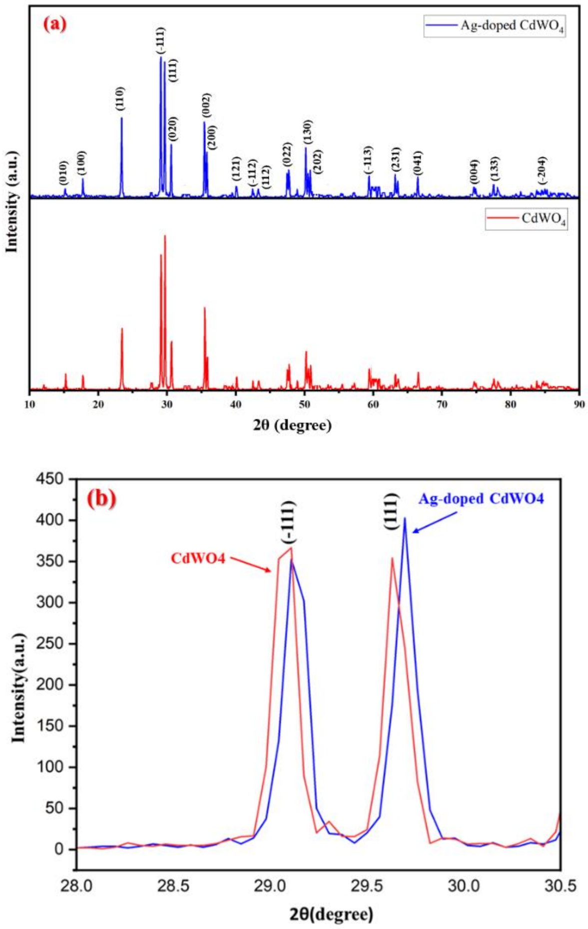

Figure 2. XRD spectra of (a): pure and Ag-doped $CdWO_4$, (b): Comparing the intensity and position of the lattice planes (-111) and (111)

3.2. FTIR

Fourier-transform infrared (FTIR) spectroscopy was conducted to analyze the bonding environments within the samples. As depicted in Fig. 3(a), the FTIR spectra of Ag-doped $CdWO_4$ nanopowder, calcined at 600°C, were measured within the wavenumber range of 400–4000 cm^{-1}. Seven vibrational modes were observed within the characteristic region of the IR spectrum (400–1400 cm^{-1}), corresponding to W–O, W–O–W, and Cd–O vibrations. Another vibrational mode was identified within the wavenumber range of 1400–4000 cm^{-1}. As illustrated in Fig. 3(b), the depth of the valley around 596 cm^{-1}, corresponding to Cd–O in-plane deformations and W–O vibrations, exhibited a slight decrease compared to the pure sample. This observation indicates that the presence of Ag^+ ions influenced both the W–O and Cd–O vibrational modes.

As shown in Figure 3(c), the intensity of W–O in-plane deformation vibrations at approximately 723 cm^{-1} and 891 cm^{-1} was lower compared to the pure sample. This reduction in intensity indicates that the presence of Ag^+ ions influenced the terminal W–O vibrations within a single octahedral structure. The valley observed around 1400 cm^{-1}, as shown in Fig. 3(d), is attributed to H–O–H stretching vibrations. The intensity of these vibrations slightly decreased, indicating interactions with the dopant ions (Dehkordi et al, 2022; Novais et al, 2018; Banari et al, 2024).

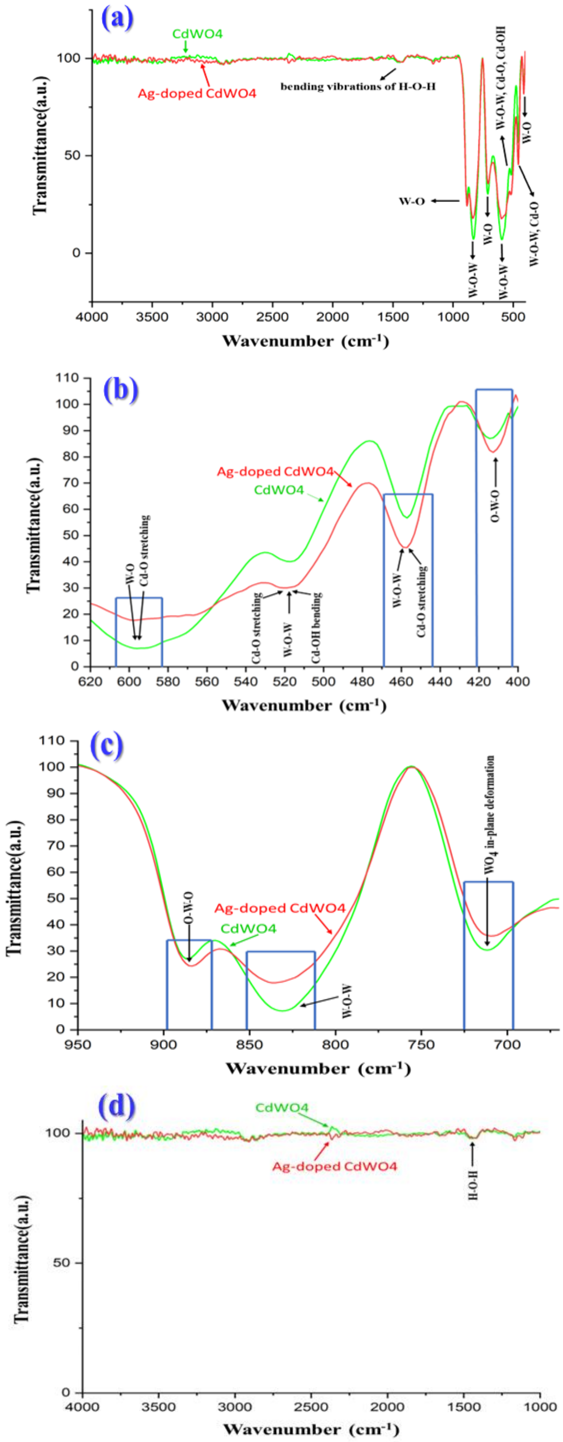

Figure 3. FTIR spectra of (a): pure and Ag-doped CWO, (b): Comparison of CWO and Ag-doped CWO in 620–400 cm^{-1}, (c): in 950–700 cm^{-1}, and (d): in 4000–1000 cm^{-1}

3.3. FESEM IMAGES

The surface structural morphology of the prepared samples was meticulously examined using field emission scanning electron microscopy (FESEM). Figures 4(a) and 4(b) present the FESEM images of the synthesized $CdWO_4$ (CWO) nanoparticles and Ag-doped $CdWO_4$ nanoparticles, respectively. It is evident that both types of nanoparticles exhibited aggregation and predominantly rod-like shapes, with a few spherical shapes observed between the rods. According to Figures 4(a) and 4(b), the mean sizes of the normal $CdWO_4$ and Ag-doped $CdWO_4$ nanoparticles are 345 nm and 267 nm, respectively. The FESEM images revealed that the particle sizes observed were notably larger than the crystallite sizes calculated using Scherer's formula.

3.4. EDX-MAPPING

Energy-dispersive X-ray spectroscopy (EDX) and elemental mapping were employed to verify the elemental composition and spatial distribution on the surface of the synthesized Ag-doped $CdWO_4$ nanoparticles. The EDX spectra, presented in Figure 5, revealed peaks corresponding to cadmium (Cd), tungsten (W), oxygen (O), and silver (Ag). These findings substantiate the successful synthesis of the target material. The atomic and mass percentages of these elements (Cd, W, O, and Ag) were derived from the peak intensities, confirming the efficacy of the synthesis and doping processes. Additionally, Figure 5 confirms the uniform dispersion of the elements within the nanoparticles.

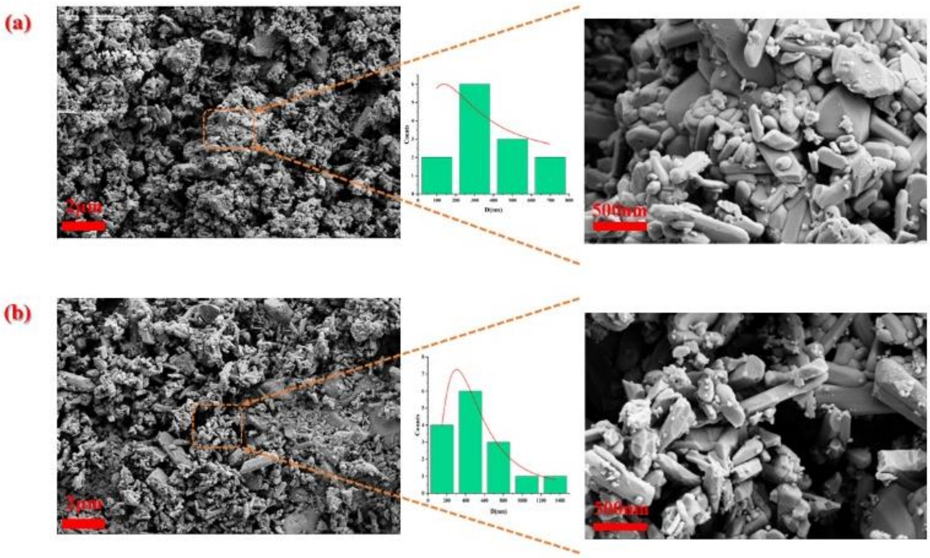

Figure 4. FESEM images and particle size distributions of (a): pure CWO, and (b): Ag-doped CWO nanoparticles

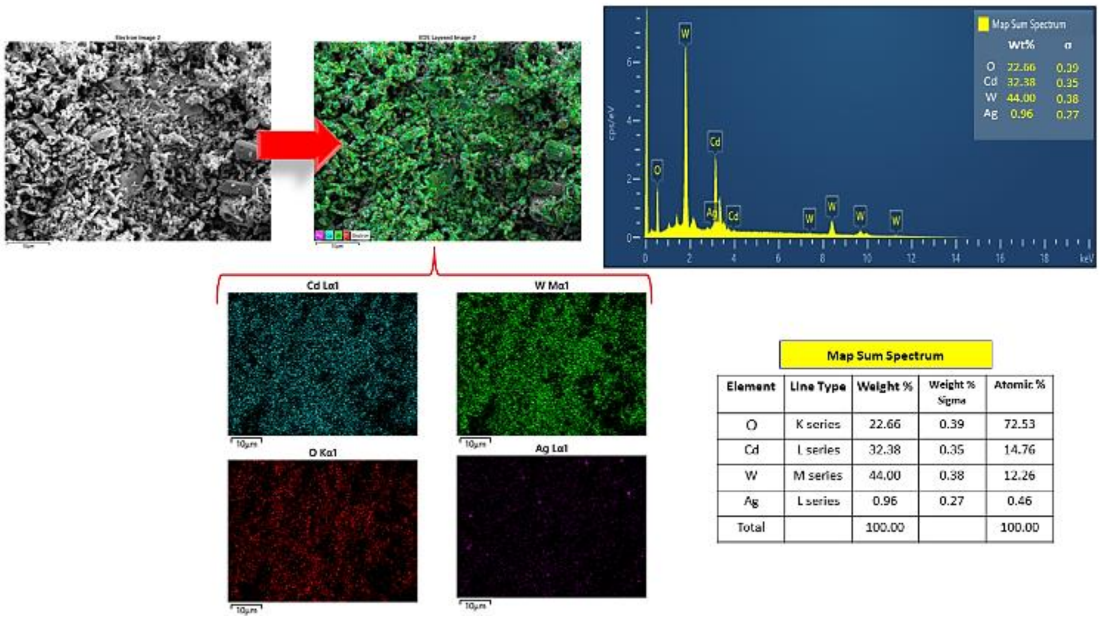

Element	Line Type	Weight %	Weight % Sigma	Atomic %
O	K series	22.66	0.39	72.53
Cd	L series	32.38	0.35	14.76
W	M series	44.00	0.38	12.26
Ag	L series	0.96	0.27	0.46
Total		100.00		100.00

Figure 5. EDAX and Map elemental of the Ag-doped CWO nanoparticles

3.5. UV–VIS

Ultraviolet-visible (UV-Vis) absorption spectra and Tauc plots were used to analyze both $CdWO_4$ and Ag-doped $CdWO_4$ nanoparticles under UV irradiation. As depicted in Figures 6(a) and 6(b), the absorption edges for $CdWO_4$ and Ag-doped $CdWO_4$ are approximately 230 nm and 220 nm, respectively.

The band gap was determined utilizing Equation 2:

$$\alpha h\nu = A(h\nu - Eg)^n \quad (2)$$

In Equation (2), the parameters hv, Eg, A, and n represent the absorption coefficient, the emitted photon energy, the bandgap energy, and the proportionality constant, respectively (Farahani et al, 2024). As indicated in Figures 6(a) and 6(b), the bandgap values for $CdWO_4$ and Ag-doped $CdWO_4$ nanopowders were determined to be 5.4 eV and 5.8 eV, respectively. Although the bandgap energy exhibited only minimal change, the introduction of surface Ag^+ created energy states below the conduction band of tungstate. The energy states of tungstate above the conduction band were higher than these new levels. Consequently, the bandgap of Ag-doped $CdWO_4$ slightly increased compared to that of pure $CdWO_4$.

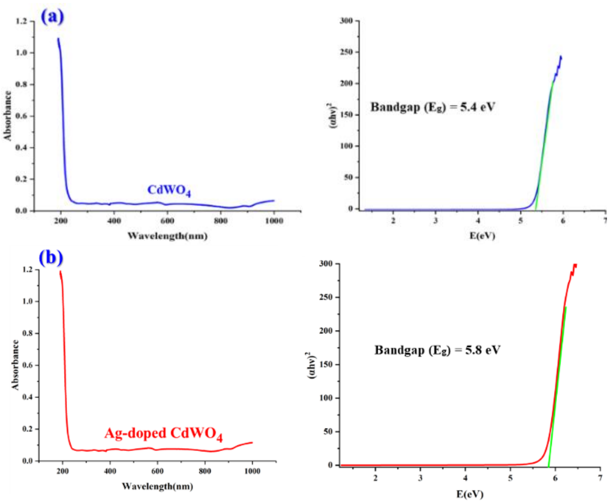

Figure 6. UV–Vis absorbance spectra and band gap energy of (a): CWO, and (b): Ag-doped CWO nanoparticles

3.6. ALPHA IRRADIATION SENSITIVITY

To assess the samples' response to alpha radiation, 1.7 g of polyvinyl alcohol (PVA) (MW = 35,000, Sigma) was dispersed in 20 mL of toluene (Merck) and stirred for 3 hours. The resulting intensely luminescent powders were thoroughly crushed. Subsequently, 1.3 g of the powders was dispersed in 5 mL of toluene, added to the polymer matrix solution, and stirred again at an elevated velocity for 3 hours. *(The mass ratio of scintillator powder to polymer was approximately 0.7.)* An appropriate quantity of the prepared material mixture was evenly distributed onto a glass plate and allowed to dry at room temperature. After 24 hours, the polymer films were easily detached and subsequently sectioned into square pieces (Novais et al, 2018; Alamdari et al, 2022). A brief schematic of the scintillation of the flexible scintillator films and the experimental setup is shown in Figure 7.

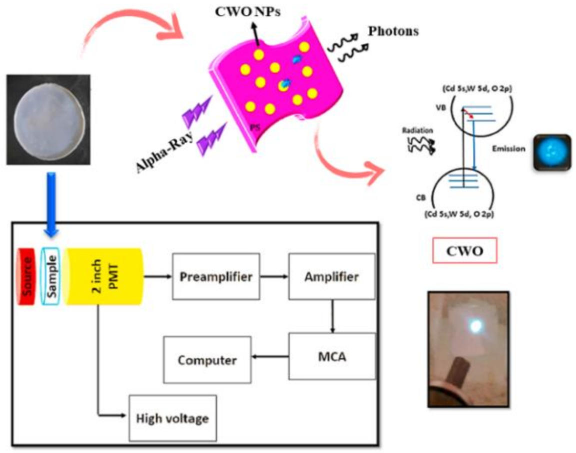

Figure 7. Schematic diagram for alpha-ray irradiation measurement setup

Figure 8 presents the pulse-height spectra of CWO, CWO:Ag, and neat PVA thin films (comprising polymer and CWO scintillation filler). The scintillation pulse-height spectra of the samples subjected to alpha irradiation indicate an increase in the count rate intensity for the CWO:Ag nanocomposite film compared to the CWO thin film. The interplay between nanoparticles and alpha particles evidently enhances the scintillation light yield in the Ag-doped CWO nanocomposite film sample.

The absolute counting efficiency (ε) of the samples was determined using Equation (3):

$$\varepsilon = \frac{r_{net}}{A} \quad (3)$$

where A represents the activity of the alpha source, and r_{net} the net counting rate (Hosseinpour et al, 2023; Alamdari et al, 2019; Dehkordi et al, 2022). The absolute efficiency values of CWO and CWO: Ag were obtained as 38%, and 57%, respectively.

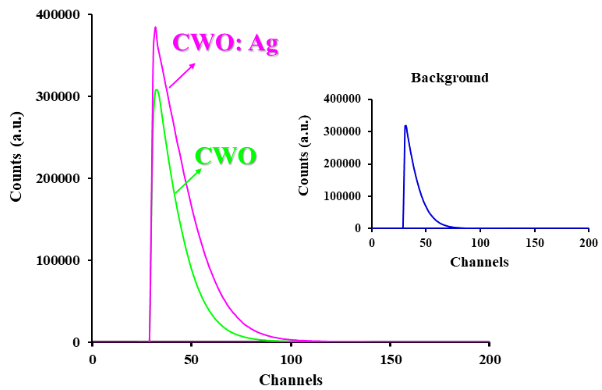

Figure 8. Pulse height spectra of PVA (background) and prepared CWO, CWO:Ag flexible films under alpha-ray irradiation (^{241}Am 5.5 MeV alpha source)

4. CONCLUSION

As previously discussed, the optoelectronic industry necessitates the advancement of novel ionizing radiation detection sensors to cater to a multitude of applications. Given the manufacturing challenges and high costs associated with single-crystal detectors, there is a pressing need to advance innovative detection methodologies and sensor technologies. The development of flexible material nanopowders through their incorporation into soft substrates represents a highly novel and promising approach for the creation of compact, portable devices. In this context, our study sought to harness the distinctive attributes of the synthesized materials $CdWO_4$ (CWO) and Ag-doped $CdWO_4$ (CWO:Ag) nanoparticles. Consequently, a straightforward and cost-effective approach was employed to fabricate CWO and CWO:Ag composite films endowed with the ability to sense ionizing radiation. The presence of the monoclinic wolframite structure was validated through X-ray diffraction (XRD) analysis. The findings revealed that the Ag-doped $CdWO_4$ (CWO:Ag) nanoparticles displayed remarkable luminescent emission properties when exposed to ultraviolet (UV) radiation. Additionally, the fabricated composite film demonstrated elevated scintillation sensitivity under exposure to ^{241}Am alpha sources. The robust photonic response of the $CdWO_4$:Ag composite layer indicates that the developed sensor holds significant promise for future applications in a variety of fields. These include flexible radiation detectors, advanced optical devices, alpha particle sensors, and X-ray imaging technologies.

ACKNOWLEDGEMENTS

The authors wish to acknowledge Semnan University for all support throughout this work. We also would like to express our sincere appreciation to Parto Negar Shahab Company -Radonik for their invaluable assistance and support in this research.

REFERENCES

1. Alamdari, S., Ghamsari, M. S., & Tafreshi, M. J. (2020). Novel scintillation properties by entrapping ZnO: Ga nanocrystals in epoxy polymer. *Progress in Nuclear Energy*, *130*, 103495. https://doi.org/10.1016/j.pnucene.2020.103495
2. Alamdari, S., Ghamsari, M. S., & Tafreshi, M. J. (2020). Optimization of Gallium concentration to improve the performance of ZnO nanopowders for nanophotonic applications. *Ceramics International*, *46*(4), 4484-4492. https://doi.org/10.1016/j.ceramint.2019.10.175
3. Alamdari, S., Ghamsari, M. S., & Tafreshi, M. J. (2025). Novel thermo-luminescent ceramics. In *Luminescent Ceramics* (pp. 211-263). Elsevier. https://doi.org/10.1016/B978-0-323-91137-5.00011-7
4. Alamdari, S., Ghamsari, M. S., Afarideh, H., Mohammadi, A., Geranmayeh, S., Tafreshi, M. J., & Ehsani, M. H. (2019). Preparation and characterization of GO-ZnO nanocomposite for UV detection application. *Optical Materials*, *92*, 243-250. https://doi.org/10.1016/j.optmat.2019.04.041
5. Alamdari, S., Haji Ebrahimi, M., Mirzaee, O., Jafar Tafreshi, M., Majlesara, M.H., Tajali, M., Sasani Ghamsari, M. and Mohammadi, A., (2022). Cerium doped Tungsten-Based Compounds for Thermoluminescence Application. *Progress in Physics of Applied Materials*, *2*(1), pp.35-40., https://doi.org/10.22075/ppam.2022.27086.1028
6. Alamdari, S., Jafar Tafreshi, M., & Sasani Ghamsari, M. (2019). Preparation and characterization of gallium-doped zinc oxide/polystyrene nanocomposite scintillator for alpha particles detection. *Applied Physics A*, *125*(6), 450. https://doi.org/10.1007/s00339-019-2727-1
7. Alamdari, S., Jafar Tafreshi, M., Sasani Ghamsari, M., & Majles Ara, M. H. (2021). Preparation and characterization of ZnO and $CdWO_4$ nanopowders for radiation sensing. *Progress in Physics of Applied Materials*, *1*(1), 14-18. https://doi.org/10.22075/ppam.2021.23502.1007
8. Alamdari, S., Majles Ara, M. H., & Tafreshi, M. J. (2022). Synthesize and optical response of ZnO/$CdWO_4$: Ce nanocomposite with high sensitivity detection of ionizing radiations, *Opt. Laser Technol.*, 151, 107990, ISSN 0030-3992, https://doi.org/10.1016/j.optlastec.2022.107990
9. Alamdari, S., Tafreshi, M. J., & Ghamsari, M. S. (2022). Highly stable Ga-doped ZnO/polystyrene nanocomposite film with narrow-band cyan emission. *Journal of Semiconductors*, *43*(12), 122301. https://doi.org/10.1088/1674-4926/43/12/122301
10. Azadmehr, S., Jafat Taftreshi, M., Alamdari, S. (2022) Synthesis, characterization and scintillation response of $ZnWO_4$-GO nanocomposite. J. Compos. Compd 4(12), 158–162. https://doi.org/10.52547/jcc.4.3.5
11. Banari, M., Memarian, N., Concina, I., & Vomiero, A. (2023). UV photodetector study based on Ce: ZnO nanostructures with different concentration of Ce dopant. *Optical Materials*, *146*, 114576. https://doi.org/10.1016/j.optmat.2023.114576
12. Banari, M., Memarian, N., Kumar, P., You, S., Vomiero, A., & Concina, I. (2024). CeO2: ZnO hybrid nanorods for self-powered UV-photodetectors. *Ceramics International*. https://doi.org/10.1016/j.ceramint.2024.10.254
13. Dehkordi, N. H., Alamdari, S., & Raeisi, M. (2022). The blue-green emission color of Ag+, Gd3+ co-activated CdWO4 phosphor via energy transfer for luminescence applications. *Physica B: Condensed Matter*, *639*, 413969. https://doi.org/10.1016/j.physb.2022.413969
14. Dehkordi, N. H., Raeisi, M., & Alamdari, S. (2022). Development of flexible scintillation sensors based on Ag and Gd doped CdWO4 nanocomposites. *Applied Radiation and Isotopes*, *189*, 110457. https://doi.org/10.1016/j.apradiso.2022.110457
15. Dehkordi, N. H., Raeisi, M., & Alamdari, S. (2022). Structure, morphology, and luminescence properties of brilliant blue-green-emitting CdW O 4: A g+ 1 and G d+ 3 phosphors for optical applications. *Journal of Nanoparticle Research*, *24*(3), 47. https://doi.org/10.1007/s11051-022-05414-6
16. Farahani, M. M. H., Hajiebrahimi, M., Alamdari, S., Najafzadehkhoee, A., Khounsaraki, G. M. , Agheb, M. & Mirzaee, O. (2024). Synthesis and antibacterial activity of silver doped zinc sulfide/chitosan bionanocomposites: A new frontier in biomedical applications, *Int. J. Biol. Macromol.*, *280*, p. 135934, https://doi.org/10.1016/j.ijbiomac.2024.135934.26
17. Hajiebrahimi, M., Alamdari, S. Mirzaee, O. & Tajally M. (2022). Luminescence Investigation of Ce Doped ZnO/$CdWO_4$ Nanocomposite. *Advanced Ceramics Progress* 8, no. 3. 8-12, https://doi.org/10.30501/acp.2022.363264.1102

18. Hemmati, M., Jafar Tafreshi, M., Ehsani, M. H. & Alamdari, S. (2022). Highly sensitive and wide-range flexible sensor based on hybrid $BaWO_4$@ CS nanocomposite." *Ceramics International* 48, no. 18 26508-26518. https://doi.org/10.1016/j.ceramint.2022.05.347

19. Hosseinpour, M., Abdoos, H., Mirzaee, O., & Alamdari, S. (2023). Fabrication and characterization of a new flexible ionizing ray sensor based on lead tungstate (PbWO4). *Ceramics International*, *49*(3), 4722-4732. https://doi.org/10.1016/j.ceramint.2022.09.362

20. Hosseinpour, M., Mirzaee, O., Alamdari, S., Menéndez, J.L., Abdoos, H.: (2023). Development of a novel flexible thin PWO(Er)/ZnO(Ag) nanocomposite for ionizing radiation sensing. *J. Alloy. Compd. 967*, 171678. https://doi.org/10.1016/j.jallcom.2023.171678

21. Madani, M., Mansourian, M., Almadari, S., Mirzaee, O., & Tafreshi, M. J. (2022). Enhanced photosensitivity of heterostructure SiO2/Bi2WO6/GO composite nanoparticles. *Physica B: Condensed Matter*, *645*, 414241. https://doi.org/10.1016/j.physb.2022.414241

22. Murphy, H.J., et al., (1999). Optical and EPR characterization of point defects in bismuthdoped $CdWO_4$ crystals. Radiat. Eff. Defect Solid 149, 273–278, 1-4. https://doi.org/10.1080/10420159908230167

23. Novais, S. M. V., Monteiro, T. J., Teixeira, V. C., Gomes, M. A., Valerio, M. E. G., Macedo, Z. S., & Barbosa, L. B. (2018). Hydrothermal synthesis of CdWO4 for scintillator-polymer composite films development. *Journal of Luminescence*, *199*, 225-231. https://doi.org/10.1016/j.jlumin.2018.03.056

24. Sahani, R. M., Kumari, C., Pandya, A., & Dixit, A. (2019). Efficient alpha radiation detector using low temperature hydrothermally grown ZnO: Ga nanorod scintillator. *Scientific reports*, *9*(1), 11354. https://doi.org/10.1038/s41598-019-47732-1

25. Tafreshi, M. J., & Alamdari, S. (2022). Facile synthesis of ZnO/CWO nanocomposite with brilliant enhanced optical response. *Applied Radiation and Isotopes*, *180*, 110050. https://doi.org/10.1016/j.apradiso.2021.110050

26. Wang, X., Wang, Y., Wang, Y., Liu, H., Zhang, Y., Liu, W., ... & Wang, S. (2020). Color-tunable X-ray scintillation based on a series of isotypic lanthanide–organic frameworks. *Chemical Communications*, *56*(2), 233-236., https://doi.org/10.1039/C9CC08114C

27. Xu, L. J., Lin, X., He, Q., Worku, M., & Ma, B. (2020). Highly efficient eco-friendly X-ray scintillators based on an organic manganese halide. *Nature communications*, *11*(1), 4329. https://doi.org/10.1038/s41467-020-18119-y

28. Ziluei, H., Azimirad, R., Larijani, M. M., & Ziaie, F. (2017). Preparation and optimization of CdWO4-polymer nano-composite film as an alpha particle counter. *Nuclear Instruments and Methods in Physics Research Section A: Accelerators, Spectrometers, Detectors and Associated Equipment*, *852*, 85-90. https://doi.org/10.1016/j.nima.2017.01.015